Research Article

Tunable temperature- and shear-responsive hydrogels based on poly(alkyl glycidyl ether)s

Christopher R Fellin,[a] Steven M Adelmund,[b] Dylan G Karis,[a] Ryan T Shafranek,[a] Robert J Ono,[a] Cecilia G Martin,[a] Trevor G Johnston,[a] Cole A DeForest[b] and Alshakim Nelson[a]*

Abstract

We describe the synthesis, characterization and direct-write 3D printing of triblock copolymer hydrogels that have a tunable response to temperature and shear stress. In aqueous solutions, these polymers utilize the temperature-dependent self-association of poly(alkyl glycidyl ether) 'A' blocks and a central poly(ethylene oxide) segment to create a physically crosslinked three-dimensional network. The temperature response of these hydrogels was dependent upon composition, chain length and concentration of the 'A' block in the copolymer. Rheological experiments confirmed the existence of sol–gel transitions and the shear-thinning behavior of the hydrogels. The temperature- and shear-responsive properties enabled direct-write 3D printing of complex objects with high fidelity. Hydrogel cytocompatibility was also confirmed by incorporating HeLa cells into select hydrogels resulting in high viabilities over 24 h. The tunable temperature response and innate shear-thinning properties of these hydrogels, coupled with encouraging cell viability results, present an attractive opportunity for additive manufacturing and tissue engineering applications.
© 2018 Society of Chemical Industry

Supporting information may be found in the online version of this article.

Keywords: hydrogel; triblock copolymer; lower critical solution temperature; shear-thinning; additive manufacturing; cytocompatibility

INTRODUCTION

Hydrogels are water-swollen, three-dimensional networks of molecules or molecular assemblies that are useful in a range of applications that include drug delivery and tissue engineering.[1–4] These hydrophilic networks are bound by chemical or physical crosslinks between the molecules.[5] Stimuli-responsive hydrogels belong to a unique class of materials that adapt to environmental cues such as pH,[6,7] temperature,[8,9] light[10,11] and mechanical impetus.[12–14] Temperature and shear stress are examples of two important stimuli responses that enable effective drug delivery,[15–17] additive manufacturing[18–20] and tissue engineering.[21–23] A thermally reversible sol–gel response – wherein the hydrogel liquefies upon cooling – allows for facile loading of a hydrogel ink and homogeneous dispersion of heat-insensitive drugs or additives in the liquid state.[24] Furthermore, shear-thinning hydrogels facilitate the formation of 3D printed objects and protect encapsulated cells from the damaging shear stress of a syringe nozzle.[25,26] These materials exist in the gel state under ambient conditions, but experience a drop in viscosity when activated by shear stress. The extruded filaments are proposed to undergo a 'plug flow' as the material travels through a nozzle.[27]

Multi-stimuli-responsive hydrogels can be formulated from aqueous solutions of amphiphilic ABA triblock copolymers comprised of at least one block that exhibits a temperature-dependent aqueous solubility known as a lower critical solution temperature (LCST). The Lewis group reported the 3D printing of one such hydrogel composed of commercially available Pluronic F127, which is a poly(ethylene oxide)-*block*-poly(propylene oxide)-*block*-poly(ethylene oxide) triblock copolymer.[28] It was demonstrated that the temperature response of Pluronic F127 hydrogels is driven by the LCST of the poly(propylene oxide) 'B' block.[29–31]

We have recently reported similar ABA triblock copolymers that incorporate poly(isopropyl glycidyl ether) (PiPGE) 'A' blocks as hydrogel inks for 3D printing.[32] These PiPGE-*block*-poly(ethylene oxide)-*block*-PiPGE triblock copolymers utilize the LCST of the PiPGE 'A' blocks to form hydrogels in aqueous solutions. These hydrogels exhibit a dual-stimuli response to temperature and shear stress similar to that of F127 but require lower polymer concentrations. Based on this research, we envisioned a poly(alkyl glycidyl ether)-*block*-poly(ethylene oxide)-*block*-poly(alkyl glycidyl ether) triblock copolymer platform with a tunable temperature response. The inherent architectural design of the triblock would retain the temperature- and shear-responsive properties demonstrated in our previous work but enable additional freedom to alter the temperature response through the incorporation of comonomers, adjustment of chain length and alteration of

* Correspondence to: A Nelson, Department of Chemistry, University of Washington, Seattle, WA 98195, USA. E-mail: alshakim@uw.edu

a Department of Chemistry, University of Washington, Seattle, WA, USA

b Department of Chemical Engineering, University of Washington, Seattle, WA, USA
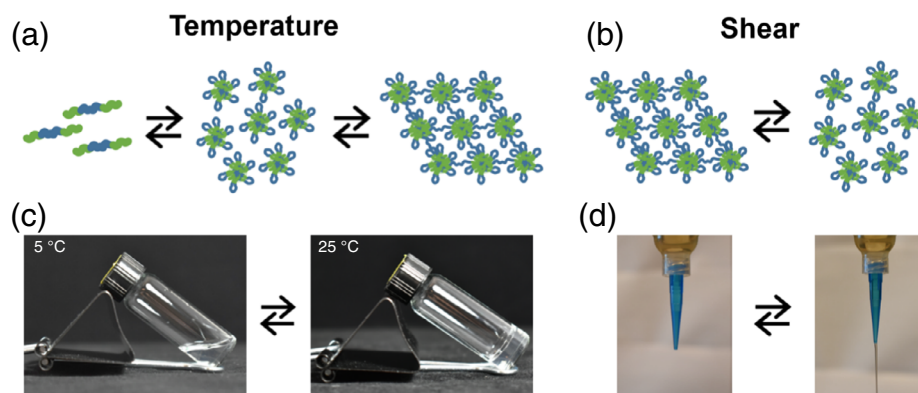
Figure 1. Graphical representations of (a) temperature-dependent equilibrium between unimers (low temperature) and a flower micelle network (high temperature) and (b) shear stress-induced breaking of physical crosslinks for the poly(alkyl glycidyl ether)-*block*-poly(ethylene oxide)-*block*-poly(alkyl glycidyl ether) triblock copolymer platform. Representative photographs that demonstrate the macroscale (c) thermo-responsive sol (5 °C) to gel (25 °C) transition and (d) extrusion-activated shear-responsive properties of a 20 wt% hydrogel of polymer **9** (0.41 mm inner diameter nozzle).

polymer concentration. We theorize that these triblock copolymers exist as individually solvated unimers at low temperatures, but form networks of physically crosslinked flower micelles at higher temperatures as the solvent becomes increasingly unfavorable for the poly(alkyl glycidyl ether) 'A' blocks.[33–36] The dynamic nature of the physical crosslinks between micelles enables a reversible response to shear stress, facilitating extrusion of these hydrogels from a syringe (Fig. 1).[37]

In order to further examine the versatility of this platform as temperature- and shear-responsive materials, we investigated a series of poly(alkyl glycidyl ether) homopolymers and poly(alkyl glycidyl ether)-*block*-poly(ethylene oxide)-*block*-poly(alkyl glycidyl ether) triblock copolymers and their corresponding hydrogels. Aqueous solutions of these polymers were examined via UV-visible spectroscopy to identify trends in cloud point temperature (T_{cp}), while phase diagrams were employed to map the physical state of the triblock copolymers at various concentrations and temperatures. A series of rheological tests were conducted to further characterize the dual-stimuli-responsive behavior of these hydrogels. Investigations into the printability and cytocompatibility of the platform indicate a promising potential for use in additive manufacturing and tissue engineering.

EXPERIMENTAL

Materials

All chemicals and solvents were purchased from Sigma-Aldrich or Fisher Scientific and used without further purification unless noted otherwise. Isopropyl glycidyl ether (iPGE; 98%), ethyl glycidyl ether (EGE; 98%), allyl glycidyl ether (AGE; 99%, Acros), methyl glycidyl ether (MGE; 85%, TCI America) and *n*-propyl glycidyl ether (synthesis detailed in supporting information) were dried over CaH_2 for 24 h, distilled into a flask containing butylmagnesium chloride (2 mol L^{-1} in tetrahydrofuran, THF), re-distilled and stored under N_2 atmosphere. Poly(ethylene oxide) (PEO; M_n of 8000 g mol^{-1}) was dried under vacuum overnight prior to use. Dry THF was obtained using neutral alumina using a Pure Process Technology solvent purification system. A potassium naphthalenide solution (1 mol L^{-1}) was prepared by dissolving naphthalene (3.2 g) in THF (25 mL), adding potassium (0.975 g), and storing under N_2 atmosphere. ^{1}H NMR spectra were obtained with a Bruker Advance 300 or 500 MHz spectrometer. Gel permeation chromatography was performed using a Waters chromatograph equipped with

two 10 μm Malvern columns (300 mm × 7.8 mm) connected in series with increasing pore size (1000, 10 000 Å), using chloroform (Optima, 0.1% (v/v) trimethylamine) as the eluent, and calibrated with PEO standards (400–40 000 g mol^{-1}). The relative molecular weights were measured in chloroform using PEO standards and a refractive index detector (flow rate: 1 mL min^{-1}).

Homopolymer synthesis

All alkyl glycidyl ether homopolymers were synthesized by utilizing the same synthetic procedure with different monomer feed ratios. The following poly(isopropyl glycidyl ether) synthetic scheme will serve as an example. The initiator 4-methylbenzyl alcohol (0.122 g, 1 mmol) was added to an oven-dried, 100 mL round-bottom flask. Potassium naphthalenide solution (1 mol L^{-1} in THF) was titrated until a light green paste was formed. The reaction flask was evacuated overnight to drive off the remaining THF. Then iPGE (6.49 mL, 51.56 mmol) was added to the dried mixture of deprotonated initiator, and the reaction was stirred at 70 °C for 45 h. The polymer solution was quenched using a degassed 1% (v/v) AcOH in MeOH solution and dialyzed against MeOH for 3 days (three solvent exchanges) using Spectra/Por regenerated cellulose tubing (molecular weight cutoff of 1.0 kDa) that was pre-soaked in water. The dialyzed polymer solution was concentrated under reduced pressure and dried in a vacuum oven for 24 h to afford a viscous, pale yellow liquid (0.8 g). ^{1}H NMR (500 MHz, CDCl$_3$; δ, ppm): 1.13–1.14 (m, —O—CH—(CH$_3$)$_2$), 2.34 (s, —Ph—CH$_3$), 3.43–3.89 (m, (—O—CH$_2$—CH(CH$_2$—O—CH—(CH$_3$)$_2$)—O—), 4.50 (s, —Ph—CH$_2$—O—), 7.13–7.14 (d, CH$_3$—*Ph*—CH$_2$—, J = 7.5 Hz), 7.21–7.22 (d, CH$_3$—*Ph*—CH$_2$—, J = 8 Hz). Molecular weights were determined using ^{1}H NMR spectroscopy by comparing the integration values of the methylbenzylic protons (2.33 ppm) to the alkyl glycidyl ether protons (1.13–1.25 ppm) or the methylene (5.2 ppm) and vinyl (5.9 ppm) protons of AGE. Homopolymer ^{1}H NMR spectra available in supporting information (Figs S9–S21 in File S1).

Triblock copolymer synthesis

ABA triblock copolymers were synthesized via anionic ring-opening polymerization. All copolymers were initiated from PEO (M_n = 8000 g mol^{-1}). The following procedure for P(iPGE-*stat*-EGE)$_{2.2k}$-*block*-PEO$_{8k}$-*block*-P(iPGE-*stat*-EGE)$_{2.2k}$ (polymer **9**) will serve as an example for a typical triblock copolymer

synthesis. PEO (10 g, 1.25 mmol) was added to the reaction vessel and dried under vacuum overnight. Dry THF (100 mL) was added under an argon atmosphere and heated to 50 °C to facilitate dissolution of the macroinitiator. Once sufficiently dissolved, a potassium naphthalenide solution (1 mol L^{-1} in THF) was titrated into the flask until the solution remained a slight green color, indicating full deprotonation of PEO hydroxyl end groups. Then iPGE (4.07 g, 35 mmol) and EGE (3.57 g, 35 mmol) were added to begin polymerization. The reaction continued for 24 h at 65 °C and was subsequently quenched with a degassed solution of 1% (v/v) AcOH in MeOH. In the polymerizations with AGE, reactions were performed at 30 °C to avoid allyl–vinyl isomerization as reported by Lynd and co-workers.[38] The reaction mixture was then precipitated into cold hexane. The polymer was collected via centrifugation (4400 rpm, 10 min) and the supernatant decanted. The product was washed twice with additional hexane and collected again in the same manner. The isolated polymer solution was dried in a vacuum oven for at least 24 h to afford an off-white solid (13.6 g). ^{1}H NMR (500 MHz, CDCl$_3$; δ, ppm): 1.13–1.15 (m, —O—CH—(CH$_3$)$_2$), 1.15–1.19 (t, —O—CH$_2$—CH$_3$, J = 7.0 Hz), 3.47–3.79 (m, —O—CH$_2$—CH$_2$—O— and —O—CH$_2$—CH(CH$_2$—O—CH$_2$—CH$_3$)—O— and —O—CH$_2$—CH(CH$_2$—O—CH—(CH$_3$)$_2$)—O—). The method used to calculate the degree of polymerization (DP) can be found in the supporting information. Triblock Copolymer ^{1}H NMR spectra available in supporting information (Figs S22–S31 in File S1).

UV-visible spectroscopy

Values of T_{cp} were determined using UV-visible spectroscopic measurements with an Agilent 8453 spectrometer. Temperature-dependent absorbance values were acquired every 0.5 °C at λ = 600 nm with a two-minute equilibration time for all samples. The polymers were dissolved in water and equilibrated at 5 °C to afford final sample concentrations of 1 wt%. T_{cp} was measured as the temperature at 50% of the absorbance increase.

Rheological measurements

Dynamic oscillatory rheological experiments were performed using a TA Instruments Discovery HR-2 rheometer equipped with a 20 mm diameter parallel-plate geometry unless otherwise specified. Samples were equilibrated in an ice bath for at least 10 min, then carefully loaded onto the Peltier plate at 5 °C. A pre-shear experiment was applied to ensure bubbles were eliminated from the sample cell. The sample was equilibrated at 21 °C for 8 min. Strain sweep experiments were performed, and all studies were conducted using a strain value in the linear viscoelastic regime. Temperature ramp experiments were performed at 1 Hz from 5 to 50 °C at 2 °C min^{-1}. Cyclic strain tests (frequency 1 Hz) were performed at 21 °C using alternating strains of 1% for 5 min and 100% for 3 min per cycle. Viscosity *versus* shear rate experiments were performed at 21 °C. The gel yield stress values were measured under oscillatory strain (frequency of 1 Hz, 21 °C) starting with an initial strain of 0.01% and converted to applied oscillatory stress.

Direct-write 3D printing of hydrogels

A modified pneumatic direct-write 3D printer was assembled based on a Tronxy P802E 3D printer kit, from Shenzen Tronxy Technology Co. The hydrogel ink was cooled to 5 °C and poured into a Nordson Optimum 10 cm^3 fluid dispensing barrel equipped with a Metcal conical (410 μm inner diameter) precision tip nozzle.

The loaded syringe was warmed to ambient temperature and pressurized using nitrogen gas (20 psi) to extrude the gel from the nozzle at 8.0 mm s^{-1}. The printer was controlled with an Arduino using Marlin firmware. The G-code file was produced with Slic3r software.

Cell viability study

Three solutions of polymer **9** (15, 20 and 26.67 wt%) in Dulbecco's modified Eagle's medium (DMEM) supplemented with 10% fetal bovine serum (FBS) and 1% streptomycin/penicillin were equilibrated at 5 °C for 3 days. HeLa cells were grown to confluency at 37 °C. The cells were rinsed with phosphate buffered saline (PBS, pH = 7.4), detached from culture plates using trypsin (0.05%) and EDTA (0.53 mmol L^{-1}), and mixed with supplemented DMEM to afford a final concentration of 10×10^6 cells mL^{-1}. To utilize the thermally reversible gel-to-sol transition, cell medium (20 μL) was combined with polymer solution (60 μL) on ice; hydrogels were formed with final concentrations of 11.25, 15 and 20 wt%. The cell/polymer medium solution (60 μL) was pipetted onto a culture plate, immersed in supplemented DMEM and incubated at 37 °C for 24 h. The sample was cooled on an ice block and mixed with a DMEM solution containing LIVE/DEAD® reagents calcein (2 μmol L^{-1}) and ethidium homodimer-1 (4 μmol L^{-1}). This solution was placed in an incubator for 30 min at 37 °C, imaged with a Leica SP8X confocal microscope and analyzed using the Fiji image processing package.

RESULTS AND DISCUSSION

Synthesis of homopolymers and characterization of LCST response

Living anionic polymerization is an effective method[39–42] for the ring-opening polymerization[38,43] of glycidyl ether derivatives to afford polymers of controlled molecular weight and dispersity. All poly(alkyl glycidyl ether)s in this investigation were synthesized via the initiation from an alcohol using potassium naphthalenide as the base. Watanabe and co-workers[44,45] previously demonstrated that poly(alkyl glycidyl ether)s show LCST behavior in aqueous solutions. Thus, we first synthesized alkyl glycidyl ether homopolymers derived from methyl, ethyl, allyl, isopropyl or *n*-propyl glycidyl ether monomer (Scheme 1) in order to characterize their LCST responses to confirm these results for comparison to the triblock copolymers to be discussed later in this section.

Polymers with molecular weights ranging from 2.1 to 24.5 kg mol^{-1} were synthesized, and 1 wt% aqueous solutions of these polymers were subjected to UV-visible spectroscopic cloud point measurements to quantify the LCST (Table 1; Fig. S1 in File S1). The LCST transition was governed by a change in the system's free energy of mixing, ΔG_{mix}, from negative to positive upon an increase in temperature.[46,47] This was due to the amphiphilic nature of the polymer in an aqueous environment. The oxygen atoms in the poly(alkyl glycidyl ether)s acted as hydrogen bond acceptors with water that enthalpically favored a mixed state. Meanwhile, the alkyl portions of the polymer contributed to an unfavorable entropic driving force associated with the hydrophobic effect.[48–50] The balance between an enthalpically favored mixed state and an entropically favored demixed state led to a temperature-dependent solubility. At lower temperatures, the enthalpic forces of the polymer dominated the system, which yielded a negative ΔG_{mix} and a transparent solution. As the temperature increased, the negative total entropy change dominated the system and the free energy of mixing became positive.
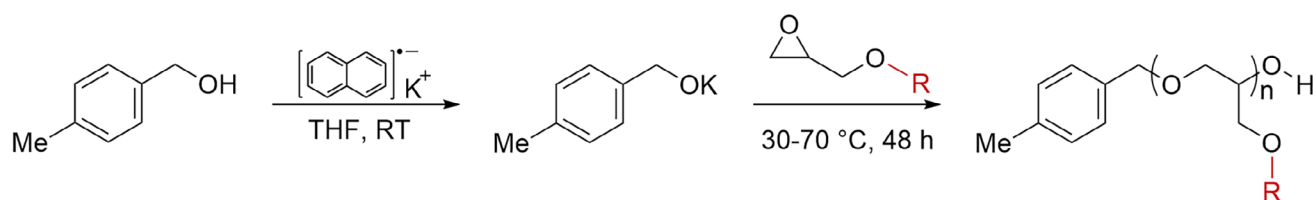
Scheme 1. Synthesis of poly(alkyl glycidyl ether)s, wherein R represents methyl, ethyl, allyl, isopropyl or *n*-propyl groups.

Table 1. Cloud point temperatures (T_{cp}) of poly(alkyl glycidyl ether)s

R group	M_n (× 10^3 g mol^{-1})[a]	Đ[b]	T_{cp} (°C)[c]
Methyl	2.1	1.14	45.0
Ethyl	3.0	1.09	10.0
Ethyl	9.5	1.12	11.1
Ethyl	24.5	1.14	10.8
Allyl	3.3	1.18	–[d]
Allyl	5.8	1.10	–[d]
Allyl	11.7	1.15	–[d]
Isopropyl	4.0	1.08	–[d]
Isopropyl	7.7	1.11	–[d]
Isopropyl	16.0	1.22	–[d]
n-Propyl	3.2	1.16	–[d]
n-Propyl	8.0	1.16	–[d]

[a] Number-average molecular weight (M_n) was determined by ^{1}H NMR spectroscopy.
[b] Dispersity (Đ) was determined by gel permeation chromatography.
[c] Cloud point temperature (T_{cp}) was determined by UV-visible spectroscopy.
[d] T_{cp} of these homopolymers could not be determined due to aqueous insolubility at all temperatures.

Phase separation occurred as the polymer chains underwent a coil-to-globule transition, and the solution became turbid.[47,48,51]

The T_{cp} values of the poly(alkyl glycidyl ether)s studied were found to abide by these thermodynamic principles and correlated inversely with the number of carbons in the R group. Hydrophilic monomers, wherein R = ethyl and methyl, displayed LCST behavior at approximately 10.8 and 45 °C, respectively. As the number of carbons in the R group increased to three (R = isopropyl, *n*-propyl and allyl), the large entropy term dominated at all temperatures and yielded water-insoluble polymers. We also observed that T_{cp} of the alkyl glycidyl ether homopolymers did not show any dependence on molecular weight, remaining nearly constant from 3.0 to 24.5 kg mol^{-1} for poly(ethyl glycidyl ether) (PEGE). These values were consistent with the results of Watanabe and co-workers[45] and Satoh and co-workers.[52] However, we noted a difference in T_{cp} observed for poly(methyl glycidyl ether) compared to a previous report by Watanabe and co-workers,[45] which was attributed to the hydrophobicity of the methylbenzyl end group that had a significant effect upon the solubility of the homopolymer as a consequence of its low molecular weight.

Synthesis of triblock copolymers and characterization of LCST response

The incorporation of different alkyl glycidyl ethers into an ABA triblock copolymer comprised of poly(alkyl glycidyl ether) 'A' blocks and a PEO 'B' block afforded a platform of polymers with a tunable temperature response. Poly(alkyl glycidyl

ether)-*block*-PEO-*block*-poly(alkyl glycidyl ether) triblock copolymers were synthesized via anionic ring-opening polymerization in THF using PEO as the macroinitiator (M_n = 8000 g mol^{-1}) and potassium naphthalenide as a base (Scheme 2).

The block length of each glycidyl ether segment was controlled by varying the molar ratio of monomer to PEO macroinitiator. Statistical copolymers were afforded by the addition of two different alkyl glycidyl ether monomers simultaneously. Specifically, EGE and AGE were copolymerized to form polymer **4**, while EGE and iPGE were copolymerized to form polymers **5**–**10**. The DP was less than the theoretical value, which suggested that homopolymer impurities or unreacted monomers were present in the reaction mixture but were removed during purification. The low dispersity values (≤1.16) of all synthesized triblock copolymers were consistent with controlled ring-opening polymerizations. The LCSTs of these polymers (Table 2) were quantified in a manner similar to the homopolymers discussed previously in this section (Figs S2 and S3 in File S1).

The thermodynamic principles that governed the LCST response of the homopolymers were also applicable to the triblock copolymers. However, the temperature-dependent aqueous solubility of the copolymer as a whole must be taken into consideration, as opposed to the solubility of the individual blocks.[52–56] Although the AGE and the iPGE homopolymers (Table 1) did not exhibit LCST behavior, the ABA triblock copolymers containing poly(allyl glycidyl ether) (PAGE) 'A' blocks (polymer **2**) or PiPGE 'A' blocks (polymer **3**) had T_{cp} values of 29.7 and 24.2 °C, respectively. Polymer **1**, which had PEGE 'A' blocks, exhibited T_{cp} at 60.0 °C. The statistical copolymerization of EGE and iPGE enabled further tuning of the LCST behavior. We successfully decreased T_{cp} of the copolymer from 60.0 °C (polymer **1**) to 46.2 °C (polymer **5**), 40.3 °C (polymer **8**) and 32.4 °C (polymer **6**) by replacing EGE units in the 'A' blocks with more hydrophobic iPGE monomers (at similar molecular weights).

In addition to molecular composition, the molecular weight of the 'A' blocks can also be exploited to tune the LCST response of the copolymer platform. To probe this relationship, the phase transition temperature of polymers **7**–**10**, with an approximately 1:1 ratio between EGE and iPGE – and with molecular weights of 1.4×10^3, 1.8×10^3, 2.2×10^3 and 2.8×10^3 g mol^{-1}, respectively – were investigated. We observed that T_{cp} of the triblock copolymer and chain length of the glycidyl ether blocks were inversely related, as the hydrophobic character of the polymer increased with the molecular weight of the poly(alkyl glycidyl ether) segments. We successfully tuned the temperature response of the triblock copolymer in water from 49.3 °C (polymer **7**) to 24.1 °C (polymer **10**) by changing the molecular weight of the 'A' block.

Triblock copolymer phase diagrams

At low concentrations (1–5 wt%), the triblock copolymer solutions became turbid as the temperature increased, due to the cloud point transition of these polymers. However, as the
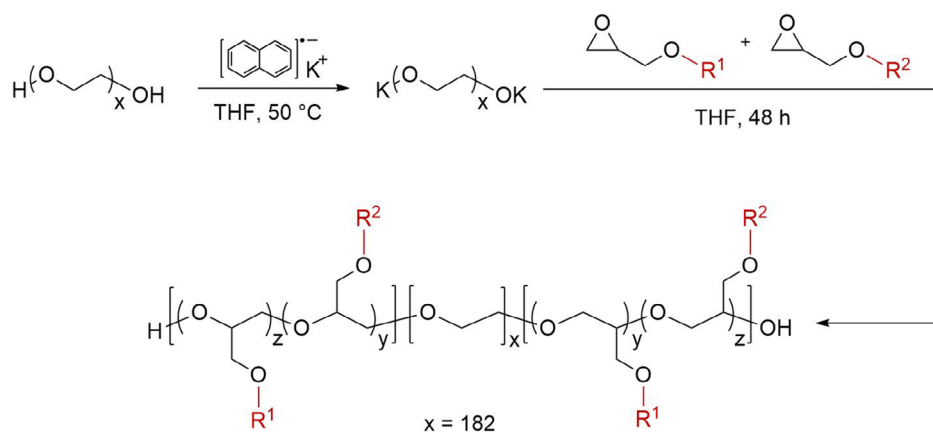
Scheme 2. Synthesis of ABA triblock copolymers, wherein R represents ethyl, allyl and isopropyl groups.

	Side chain (R_1/R_2)	M_n ($\times 10^3$ g mol^{-1})[a]	DP (z/y)[a]	$Đ$[b]	T_{cp} (°C)[c]
Table 2. Characteristics of poly(alkyl glycidyl ether)-*block*-PEO-*block*-poly(alkyl glycidyl ether) triblock copolymers					
Polymer **1**	Ethyl	1.5-*b*-8-*b*-1.5	14.8	1.10	60.0
Polymer **2**	Allyl	1.4-*b*-8-*b*-1.4	12.4	1.11	29.7
Polymer **3**	Isopropyl	1.8-*b*-8-*b*-1.8	15.2	1.16	24.2
Polymer **4**	Ethyl/allyl	1.7-*b*-8-*b*-1.7	5.6/9.6 (15.2)	1.11	43.1
Polymer **5**	Ethyl/isopropyl	1.7-*b*-8-*b*-1.7	10.6/5.0 (15.6)	1.11	46.2
Polymer **6**	Ethyl/isopropyl	1.7-*b*-8-*b*-1.7	5.4/10.2 (15.6)	1.16	32.4
Polymer **7**	Ethyl/isopropyl	1.4-*b*-8-*b*-1.4	6.5/6.3 (12.8)	1.15	49.3
Polymer **8**	Ethyl/isopropyl	1.8-*b*-8-*b*-1.8	8.2/7.9 (16.1)	1.12	40.3
Polymer **9**	Ethyl/isopropyl	2.2-*b*-8-*b*-2.2	9.8/9.9 (19.7)	1.11	31.3
Polymer **10**	Ethyl/isopropyl	2.8-*b*-8-*b*-2.8	12.6/12.7 (25.3)	1.14	24.1

[a] Number-average molecular weight (M_n) and degree of polymerization (DP) were determined by ^{1}H NMR spectroscopy.
[b] Dispersity ($Đ$) was determined by gel permeation chromatography.
[c] Cloud point temperature (T_{cp}) was determined by UV-visible spectroscopy.

polymer concentration increased ($\geq$5 wt%), this phase separation mechanism gave way to the formation of a three-dimensional hydrogel network and a sol–gel transition. To better understand the role of temperature, polymer concentration, chain length and composition in the formation of the polymer hydrogels, qualitative phase diagrams were produced for each triblock copolymer. Polymer solutions (2–30 wt%) were prepared and incubated at temperatures that ranged from 5 to 50 °C. Their physical states were determined using the vial inversion method and recorded as a transparent/opaque liquid, viscous solution or gel. Transparent formulations were clear, with no turbidity present, whereas opaque solutions were turbid and optically cloudy in appearance.

In the same manner that the hydrophobicity of the copolymers was utilized to tune T_{cp}, we exploited the inherent differences in hydrophobic character of the alkyl glycidyl ether monomers to alter the sol–gel transition temperature. Polymer **1** afforded solutions that only became a gel at temperatures >50 °C and concentrations >30 wt% as a consequence of the hydrophilicity of the PEGE block. Relative to polymer **1**, polymers **5**, **8**, **6** and **3** had a greater hydrophobic character due to the presence of iPGE units in the copolymer. We successfully formulated solutions of polymers **5**, **8**, **6** and **3** that gelled at progressively lower temperatures and concentrations relative to polymer **1** (Fig. 2).

For example, 20 wt% solutions of polymers **5**, **8**, **6** and **3** exhibited a sol–gel transition at 45, 30, 25 and 10 °C, respectively. The solubility of polymer **3** (with PiPGE 'A' blocks) significantly decreased,

such that it was not fully soluble at 30 wt%. The AGE-containing polymers afforded brittle hydrogels (Fig. S4 in File S1) and were not further investigated.

The sol–gel transition of these polymers in aqueous solution was also affected by molecular weight and polymer concentration. The sol–gel transition temperature was tuned by altering the molecular weight of the glycidyl ether 'A' blocks (Fig. 3). As the polymer chain length increased, the hydrophobicity of the polymer also increased. For polymers **7**–**10** at identical concentrations in water (20 wt%), the sol–gel transition temperature decreased as the molecular weight was increased (40, 30, 20 and 15 °C, respectively). Thus, a 25 °C range in gelation temperature was accomplished with the inclusion of 12.5 additional glycidyl ether repeat units per block. The polymer concentration also served an important role in the tunability of the gelation temperature. The sol–gel transition of each hydrogel decreased as the polymer concentration increased (Fig. 3). For example, the sol–gel transition temperature of polymer **7** was altered from 40 to 25 °C as the concentration was increased from 20 to 30 wt%.

Although the gelation temperature of these solutions cannot be directly predicted by the T_{cp} values, we observed that they were dictated by the polymer composition, molecular weight and concentration in aqueous media. These results are consistent with that reported by Georgiou and co-workers, whom obtained[57–60] similar results for their thermo-responsive methacrylate-based terpolymers. Similarly, Pluronic F127 has a reported[61] sol–gel
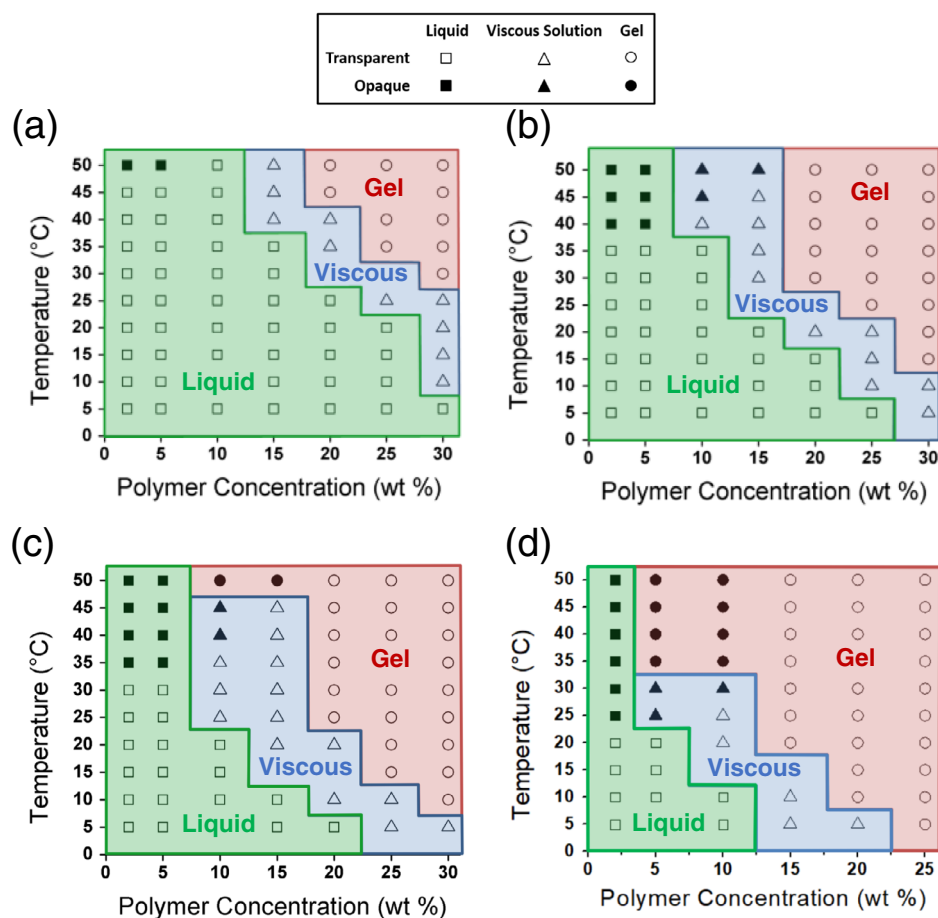
Figure 2. Temperature–concentration phase diagrams summarizing the solution and hydrogel states of triblock copolymers of the same total block length containing (a) 5.0 iPGE units (polymer **5**), (b) 7.9 iPGE units (polymer **8**), (c) 10.2 iPGE units (polymer **6**) and (d) 15.2 iPGE units (polymer **3**). The green/blue/red shaded areas indicate formulations existing as transparent/opaque liquids (□/■), viscous solutions (△/▲) and gels (○/●), respectively. Transparent formulations are clear with no turbidity. Opaque formulations are turbid and optically cloudy. Their physical states were determined using the vial inversion method.

transition (14–40 °C) that is dependent upon concentration, but has T_{cp} above 100 °C.[62] These findings stand in contrast to the PNiPAAm-*block*-PEO-*block*-PNiPAAm triblock copolymers studied by Teodorescu and co-workers, wherein the cloud point measurements and the vial inversion gelation temperatures occurred at similar temperatures.[63,64]

Triblock copolymer hydrogel rheology

Temperature- and shear-responsive hydrogels are useful for direct-write 3D printing as fugitive inks[65,66] and in the fabrication of composite hydrogels.[67] Rheometric characterization of the viscoelastic behaviors of hydrogels can serve as a screening protocol for the suitability of the hydrogels as inks for direct-write 3D printing.[28,68] Specifically, yield stress values can be used to compare the relative extrudability of hydrogels from a nozzle during the printing process. A hydrogel ink maintains a gel state below its yield stress, but the gel network is broken at stresses above this value causing the ink to flow and a steep drop in modulus. The phase diagrams in Figs 2 and 3 were utilized to identify the optimal hydrogels to investigate as inks for direct-write 3D printing. The selected hydrogels were gels at ambient temperature but reversibly transformed into the 'liquid' or 'viscous solution' state upon cooling.

Oscillatory stress ramp experiments (Fig. 4(a)) were used to determine the yield stress of these select hydrogel formulations. The 20 wt% solutions of polymers **9**, **10** and **3** had yield stress values of 569, 1200 and 1252 Pa, respectively. Hydrogels derived from polymer **9** were found to be particularly well suited for direct-write 3D printing, whereas the yield stress for hydrogels of polymers **10** and **3** were too high and the materials were more difficult to extrude. Thus, a 20 wt% formulation of polymer **9** was chosen for all further rheological experiments, as well as the direct-write 3D printing of the structures presented later in this section.

Temperature-dependent sol–gel transitions in hydrogel inks are advantageous for the addition and homogeneous distribution of additives and the transfer of these inks into the printer cartridge (syringe). The temperature-dependent viscoelastic characterization (Fig. 4(b)) confirmed the presence of a sol–gel transition as defined by the intersection of elastic (G') and viscous (G'') moduli (the rheometrical gelation temperature (T_{gel}) = 18.72 °C). At temperatures below T_{gel}, G'' exceeded G' and the polymer solution was free-flowing; above T_{gel}, G' exceeded G'' and the solution became a gel with a maximum G' of 33.3 kPa. Additional rheological characterization demonstrated the shear-thinning and self-healing properties of these hydrogels governed by the physical crosslinking of the low-T_g poly(alkyl glycidyl ether) blocks. The shear-thinning
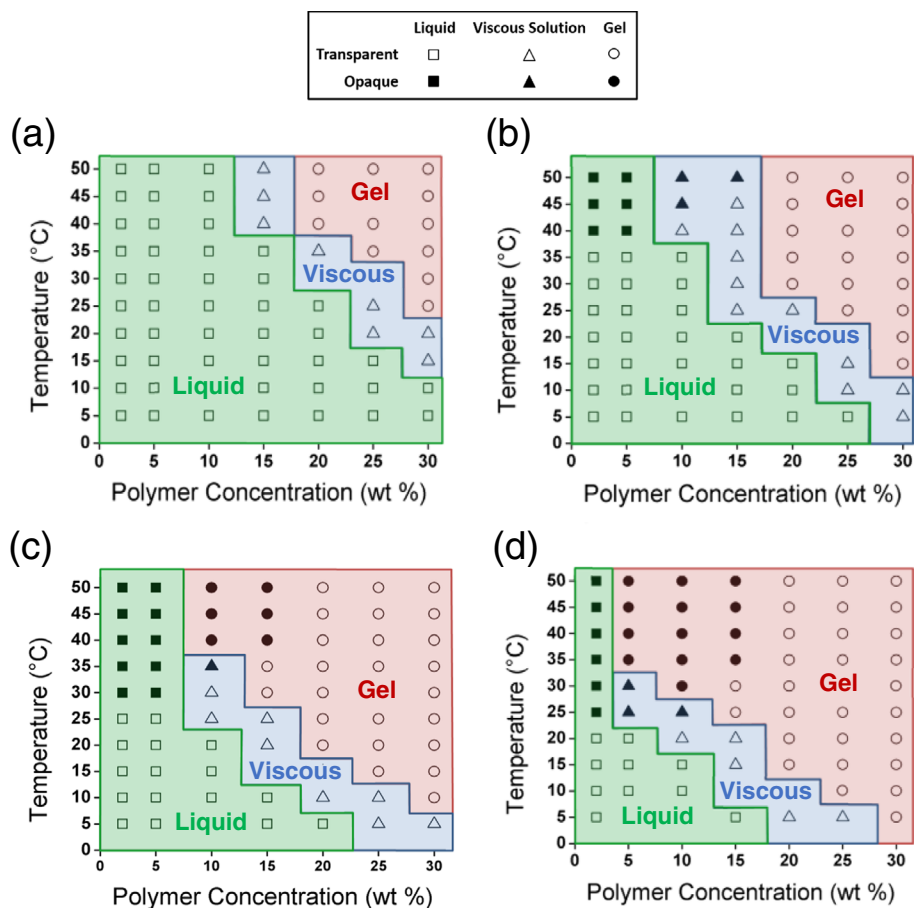
Figure 3. Temperature–concentration phase diagrams summarizing the solution and hydrogel states of triblock copolymers with increasing DP: (a) 12.8 (polymer **7**), (b) 16.1 (polymer **8**), (c) 19.7 (polymer **9**) and (d) 25.3 (polymer **10**). The green/blue/red shaded areas indicate transparent/opaque liquids (□/■), viscous solutions (△/▲) and gels (○/●), respectively. Transparent formulations are clear with no turbidity. Opaque formulations are turbid and optically cloudy. Their physical states were determined using the vial inversion method.

behavior was reflected by the decrease in viscosity with increasing shear rate (Fig. 4(c)). A dynamic oscillatory strain experiment (Fig. 4(d)) revealed a rapid and reversible response of G′ and G″ of the hydrogel to consecutive cycles of high (100%) and low (1%) strain. During periods of high strain, G″ was greater than G′, which indicated that the material was able to flow. In contrast, the sample was a gel when subjected to periods of low strain, as indicated by the larger value for G′ relative to G″. Also, G′ was nearly fully recovered after every cycle with a low degree of mechanical hysteresis.

Direct-write 3D printing

As a demonstration of the printability of our hydrogel platform, a hydrogel ink comprised of 20 wt% polymer **9** was extruded by a direct-write 3D printer. The hydrogel was loaded into the printer syringe in its liquid state at 5 °C and was then warmed to ambient temperature. The hydrogel ink was extruded through a 0.41 mm inner diameter nozzle at 20 psi and an 8.0 mm s⁻¹ print speed. During the direct-write 3D printing process, multiple layers are sequentially printed in a layer-by-layer manner. The printed objects shown in Fig. 5 had 15 layers and exhibited excellent shape fidelity with no sagging or deformation of the individual layers.

Cell viability

The cytocompatibility of hydrogels based on poly(alkyl glycidyl ether) block copolymers were investigated using HeLa cells. Hydrogels derived from polymer **9** were formulated using DMEM supplemented with 10% fetal bovine serum and 1% streptomycin–penicillin. The hydrogels in media exhibited a temperature-dependent sol–gel transition – wherein the sample became liquid upon cooling in an ice bath. This temperature-responsive feature enabled the uniform incorporation and distribution of HeLa cells in the liquid state prior to warming the solution to its gel state. The HeLa-embedded hydrogels were incubated at 37 °C for 24 h at final polymer concentrations of 11.25, 15 and 20 wt%. Cell viability was quantified via LIVE/DEAD® assay and confocal microscopy (Fig. 6). These measurements were performed in triplicate (Figs S5–S8 in File S1) and afforded viabilities of 91 (±4.10)%, 93 (±6.27)% and 84 (±18.24)%, respectively. The results of these experiments indicate acceptable cell viability at all concentrations tested and demonstrate a promising potential for use in cell encapsulation applications such as cell therapeutics and tissue engineering.

CONCLUSIONS

In summary, we have developed a highly tunable, biocompatible ABA triblock copolymer platform that utilized the hydrophobic self-association of poly(alkyl glycidyl ether) 'A' blocks in aqueous solutions to form three-dimensional networks composed of flower micelles that responded to both thermal and shear stimuli. The
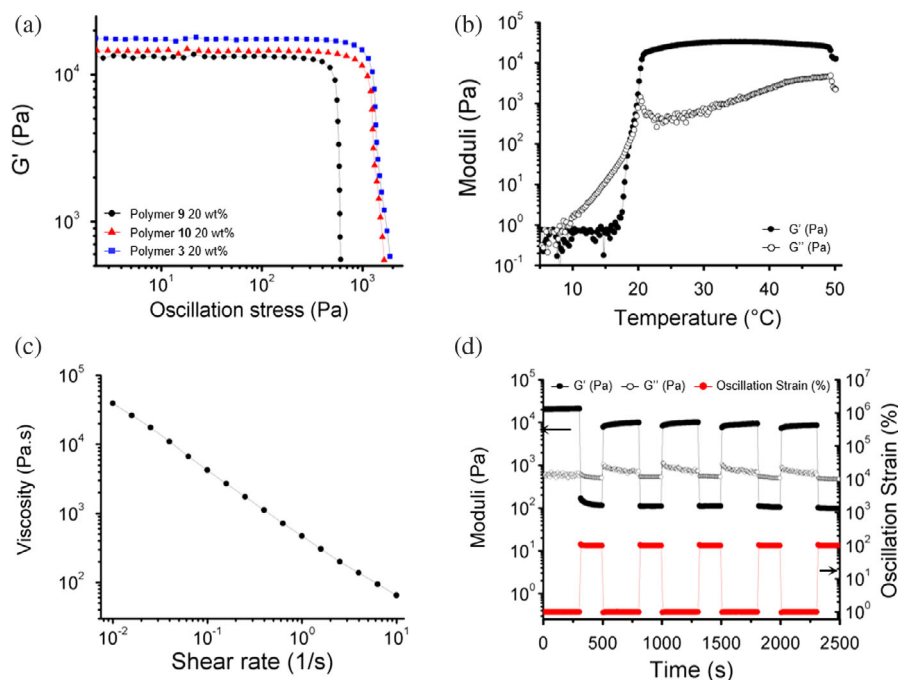
Figure 4. Rheological experiments. (a) Oscillatory stress experiment indicating yield stress. Yield stress values = 569, 1200 and 1252 for 20 wt% solutions of polymer **9**, **10** and **3**, respectively. (b) Dynamic oscillatory temperature ramp displaying elastic (G', filled) and viscous (G'', open) moduli. T_{gel} = 18.72 °C. (c) Viscosity *versus* shear rate experiment depicting shear-thinning behavior by a decrease in viscosity with increasing shear rate and. (d) Cyclic strain experiment demonstrating rapid recovery of hydrogel elastic modulus (black circles) from periods of high (100%) to low (1%) oscillatory strain (red circles). Arrows indicate reference axis; elastic/viscous moduli (left axis) and oscillatory strain (right axis).
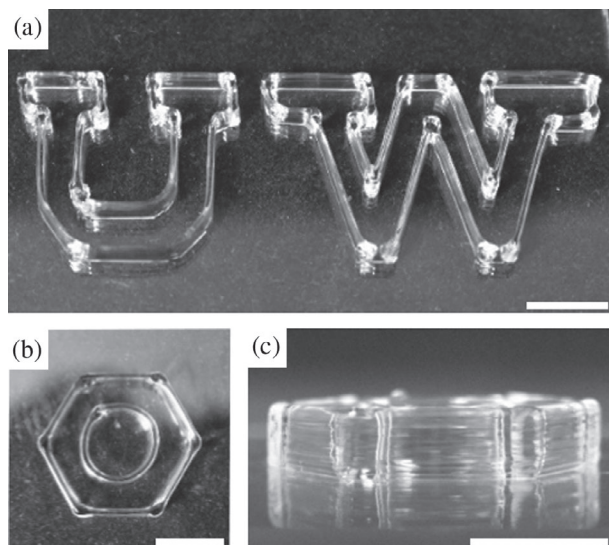
Figure 5. 3D printed structures of a 15-layer (a) University of Washington initials and (b, c) benzene ring produced using a 0.41 mm inner diameter nozzle at 8.0 mm s^{-1}. This structure was printed with a formulation of polymer **9** at 20 wt% using a pneumatic direct-write 3D printer (scale bars: 1 cm).

Figure 6. (a) Evaluation of a LIVE/DEAD® assay performed on three polymer **9** hydrogels at different concentrations (11.25, 15, 20 wt%). (b) Composite channel confocal microscopy image of encapsulated HeLa cells (11.25 wt%) (scale bar: 1000 μm).

identity of the alkyl side-chain (ethyl, isopropyl, *n*-propyl and allyl) on the poly(alkyl glycidyl ether) block played a significant role in the temperature-responsive behaviors. Interestingly, the three-carbon alkyl groups afforded homopolymers that did not exhibit any temperature response, but yielded ABA triblock copolymers which clearly exhibited temperature-dependent gelation. Copolymers comprised of ethyl and isopropyl glycidyl ethers were investigated to further tune the temperature

response. The gelation temperature of this platform can be readily tuned between 10 and 45 °C by altering the molecular composition, molecular weight, and concentration of the polymer. The temperature- and shear-responsive natures of the triblock copolymer hydrogels were characterized via phase diagrams and rheology. We also demonstrated that these polymers were suitable as inks for direct-write 3D printing to afford free-standing, multi-layered three-dimensional constructs. These stimuli-responsive hydrogels represent a promising platform to develop new materials for additive manufacturing and tissue engineering.

ACKNOWLEDGEMENTS

SUPPORTING INFORMATION
Supporting information may be found in the online version of this article.

REFERENCES

1 Malmsten M, *Soft Matter* **2**:760 (2006).
2 Alvarado-Velez M, Pai SB and Bellamkonda RV, *IEEE Trans Biomed Eng* **61**:1474–1481 (2014).
3 Nicodemus GD and Bryant SJ, *Tissue Eng B* **14**:149–165 (2008).
4 DeForest CA and Anseth KS, *Annu Rev Chem Biomol Eng* **3**:421–444 (2012).
5 Peppas NA, Hilt JZ, Khademhosseini A and Langer R, *Adv Mater* **18**:1345–1360 (2006).
6 Suhag D, Bhatia R, Das S, Shakeel A, Ghosh A, Singh A *et al.*, *RSC Adv* **5**:53963–53972 (2015).
7 Hibbins AR, Kumar P, Choonara YE, Kondiah PPD, Marimuthu T, du Toit LC *et al.*, *Polymers (Basel)* **9**:474 (2017).
8 Hatefi A and Amsden B, *J. Control Release* **80**:9–28 (2002).
9 Huang X and Lowe TL, *Biomacromolecules* **6**:2131–2139 (2005).
10 Zhao Y-L and Stoddart JF, *Langmuir* **25**:8442–8446 (2009).
11 Ter Schiphorst J, Coleman S, Stumpel JE, Ben Azouz A, Diamond D and Schenning APHJ, *Chem Mater* **27**:5925–5931 (2015).
12 Yesilyurt V, Webber MJ, Appel EA, Godwin C, Langer R and Anderson DG, *Adv Mater* **28**:86–91 (2016).
13 Jaspers M, Dennison M, Mabesoone MFJ, MacKintosh FC, Rowan AE and Kouwer PHJ, *Nat Commun* **5**:5808 (2014).
14 Badeau BA, Comerford MP, Arakawa CK, Shadish JA and DeForest CA, *Nat Chem* **10**:251–258 (2018).
15 Gupta D, Tator CH and Shoichet MS, *Biomaterials* **27**:2370–2379 (2006).
16 Li J and Loh XJ, *Adv Drug Deliv Rev* **60**:1000–1017 (2008).
17 Wang Q, Wang J, Lu Q, Detamore MS and Berkland C, *Biomaterials* **31**:4980–4986 (2010).
18 Celikkin N, Simó Padial J, Costantini M, Hendrikse H, Cohn R, Wilson C *et al.*, *Polymers (Basel)* **10**:555 (2018).
19 Highley CB, Rodell CB and Burdick JA, *Adv Mater* **27**:5075–5079 (2015).
20 Censi R, Schuurman W, Malda J, di Dato G, Burgisser PE, Dhert WJA *et al.*, *Adv Funct Mater* **21**:1833–1842 (2011).
21 Chenite A, Chaput C, Wang D, Combes C, Buschmann M, Hoemann C *et al.*, *Biomaterials* **21**:2155–2161 (2000).
22 Garty S, Kimelman-Bleich N, Hayouka Z, Cohn D, Friedler A, Pelled G *et al.*, *Biomacromolecules* **11**:1516–1526 (2010).
23 Wang Q, Wang L, Detamore MS and Berkland C, *Adv Mater* **20**:236–239 (2008).
24 Jones M-C and Leroux J-C, *Eur J Pharm Biopharm* **48**:101–111 (1999).
25 Aguado BA, Mulyasasmita W, Su J, Lampe KJ and Heilshorn SC, *Tissue Eng A* **18**:806–815 (2012).
26 Yan C, Altunbas A, Yucel T, Nagarkar RP, Schneider JP and Pochan DJ, *Soft Matter* **6**:5143 (2010).
27 Wang S, Lee JM and Yeong WY, *Int J Bioprint* **1**:3–14 (2015).
28 Kolesky DB, Truby RL, Gladman AS, Busbee TA, Homan KA and Lewis JA, *Adv Mater* **26**:3124–3130 (2014).
29 Mortensen K, *J Phys Condens Matter* **8**:A103–A124 (1999).
30 Prud'homme RK, Wu G and Schneider DK, *Langmuir* **12**:4651–4659 (1996).
31 Alexandridis P, Holzwarthf JF and Hatton TA, *Macromolecules* **27**:2414–2425 (1994).
32 Zhang M, Vora A, Han W, Wojtecki RJ, Maune H, Le ABA *et al.*, *Macromolecules* **48**:6482–6488 (2015).
33 Chu B, Liu T, Wu C, Zhou Z and Mark Nace V, *Macromol Symp* **118**:221–227 (1997).
34 Nguyen-Misra M and Mattice WL, *Macromolecules* **28**:1444–1457 (1995).
35 Baleara NP, Tirrell M and Lodge TP, *Macromolecules* **24**:1975–1986 (1991).
36 Kumi BC, Hammouda B and Greer SC, *J Colloid Interface Sci* **434**:201–207 (2014).
37 Guvendiren M, Lu HD and Burdick JA, *Soft Matter* **8**:260–272 (2012).
38 Rodriguez CG, Ferrier RC, Helenic A and Lynd NA, *Macromolecules* **50**:3121–3130 (2017).
39 Lee BF, Wolffs M, Delaney KT, Sprafke JK, Leibfarth FA, Hawker CJ *et al.*, *Macromolecules* **45**:3722–3731 (2012).
40 Satoh Y, Miyachi K, Matsuno H, Isono T, Tajima K, Kakuchi T *et al.*, *Macromolecules* **49**:499–509 (2016).
41 Lee BF, Kade MJ, Chute JA, Gupta N, Campos LM, Fredrickson GH *et al.*, *J Polym Sci A: Polym Chem* **49**:4498–4504 (2011).
42 Herzberger J, Niederer K, Pohlit H, Seiwert J, Worm M, Wurm FR *et al.*, *Chem Rev* **116**:2170–2243 (2016).
43 Yahiaoui A, Hachemaoui A and Belbachir M, *J Appl Polym Sci* **113**:535–540 (2009).
44 Ogura M, Tokuda H, Imabayashi SI and Watanabe M, *Langmuir* **23**:9429–9434 (2007).
45 Aoki S, Koide A, Imabayashi S and Watanabe M, *Chem Lett* **31**:1128–1129 (2002).
46 Klouda L and Mikos AG, *Eur J Pharm Biopharm* **68**:34–45 (2008).
47 Aseyev V, Tenhu H and Winnik FM, *Adv Polym Sci* **242**:29–89 (2011).
48 Southall NT, Dill KA and Haymet ADJ, *J Phys Chem B* **106**:521–533 (2002).
49 Chandler D, *Nature* **437**:640–647 (2005).
50 Magenau AJD, Richards JA, Pasquinelli MA, Savin DA and Mathers RT, *Macromolecules* **48**:7230–7236 (2015).
51 Schild HG, *Prog Polym Sci* **17**:163–249 (1992).
52 Isono T, Miyachi K, Satoh Y, Sato S, Kakuchi T and Satoh T, *Polym Chem* **8**:5698–5707 (2017).
53 Halacheva S, Rangelov S and Tsvetanov C, *Macromolecules* **39**:6845–6852 (2006).
54 Lutz JF and Hoth A, *Macromolecules* **39**:893–896 (2006).
55 Reinicke S, Schmelz J, Lapp A, Karg M, Hellweg T and Schmalz H, *Soft Matter* **5**:2648–2657 (2009).
56 Schilli CM, Zhang M, Rizzardo E, Thang SH, Chong YK, Edwards K *et al.*, *Macromolecules* **37**:7861–7866 (2004).
57 Ward MA and Georgiou TK, *J Polym Sci Part A Polym Chem* **48**:775–783 (2010).
58 Ward MA and Georgiou TK, *Soft Matter* **8**:2737–2745 (2012).
59 Constantinou AP and Georgiou TK, *Polym Chem* **7**:2045–2056 (2016).
60 Ward MA and Georgiou TK, *Polym Chem* **4**:1893–1902 (2013).
61 Geng H, Song H, Qi J and Cui D, *Nanoscale Res Lett* **6**:312 (2011).
62 Alexandridis P and Alan Hatton T, *Colloids Surf A* **96**:1–46 (1995).
63 Teodorescu M, Negru I, Stanescu PO, Drghici C, Lungu A and Sârbu A, *React Funct Polym* **70**:790–797 (2010).
64 Negru I, Teodorescu M, Stçănescu PO, Drăghici C, Lungu A and Sârbu A, *Colloid Polym Sci* **291**:2523–2532 (2013).
65 Homan KA, Kolesky DB, Skylar-Scott MA, Herrmann J, Obuobi H, Moisan A *et al.*, *Sci Rep* **6**:34845 (2016).
66 Kolesky DB, Homan KA, Skylar-Scott MA and Lewis JA, *Proc Natl Acad Sci USA* **113**:3179–3184 (2016).
67 Basu A, Saha A, Goodman C, Shafranek RT and Nelson A, *ACS Appl Mater Interfaces* **9**:40898–40904 (2017).
68 Smith PT, Basu A, Saha A and Nelson A, *Polymer* **152**:42–50 (2018).